

THE STUDY OF THE INFLUENCE OF PARTICLE SIZES ON THE THERMAL DECOMPOSITION OF MINERALS PRESENT IN SOLID FUEL

VITALY YU. ZAKHAROV

Department of Experimental Physics, Leningrad Polytechnic Institute, Leningrad (U.S.S.R.)

(Received 11 July 1988)

ABSTRACT

The results are presented of an experimental investigation into the influence of single particle sizes on the thermal decomposition of the natural minerals forming the mineral matter of solid fuels. The kinetic region is determined for each of the minerals.

LIST OF SYMBOLS

T	temperature
T_{\max}	temperature of reaction rate maximum
T_f	final temperature
ΔT	reaction interval
t	time
α	fraction reacted
α_{\max}	fraction reacted, corresponding to reaction rate maximum
V_d	diffusion rate
V_r	chemical reaction rate
q	heating rate
d	diameter of the sample particles
d_{cr}	critical diameter of the sample particles, at which the diffusion complications begin to emerge
d_{pr}	diameter of the sample particles, up to which it is still possible to use the kinetic equations for practical engineering calculations
ρ	density of the particles

INTRODUCTION

In the fields of power generation and power technology, the use of low-grade high-ballasted fuels with a high content of mineral matter is

increasing in a number of countries. There are enormous deposits of oil shale, for example the Green River deposits in the U.S.A. and the Pribaltic shale in the U.S.S.R., which can be described as this kind of fuel. The mineral content of Pribaltic shale reaches 70%, and it is the behaviour of the mineral matter at high temperatures that determines the fuel behaviour as a whole, as well as the technology of its exploitation. To predict the mineral matter behaviour, it is necessary to describe the thermal decomposition kinetics of all the basic minerals comprising the mineral matter. But first the limits of the application of the kinetic equations must be determined, i.e. the boundaries of the kinetic region of the reactions taking place and the particle size dependence; serious errors can be introduced without this information.

We have studied the minerals comprising the mineral matter of Pribaltic shale: calcite, magnesite (crystalline and amorphous), siderite, dolomite, kaolinite, muscovite, limonite, pyrite and gypsum. These same minerals form the basis of the mineral matter and occur in other fuels.

There are many publications devoted to the description of the thermal decomposition processes of carbonates and clay minerals; refs. 1–3 include good reviews of original works. It has been noted that, in general, the initial and final decomposition temperatures decrease with a decrease in the particle size, and also that the kinetic parameters depend on the particle size. But, as far as we know, the dependence of the kinetic region boundaries on particle size has not been determined for the process of thermal decomposition of the above minerals.

EXPERIMENTAL

The samples were milled in a laboratory roller mill and separated into the following fractions: 0–25, 25–56, 56–100, 100–150, 150–200, 250–300, 300–400, 400–500, 500–600, 600–800, 800–1000, 1000–1250, 1250–1500, 1500–1750, 1750–2000, 2000–2500, 2500–3000, 3000–3500, 3500–4000, 4500–5000 and 5000–6000 μm .

Because of the nature of the minerals studied, some of the particles contained significant levels of outside inclusions; these particles were removed from each fraction using a microscope. The chemical and X-ray analyses of the samples were then carried out. In the experiments that follow, we generally used samples with an impurity content of less than 5 wt.%. The impurity content in the coarse fractions occasionally reached 9 wt.%. Samples containing 10 or more wt.% of impurities were not used for the experiments, coarse fractions of siderite with a particle diameter $d > 3000$ μm , for which the impurity content occasionally reached 13–14 wt.%, being the exception. The results of the chemical analysis of the samples are presented in Table 1.

TABLE 1
Chemical composition of samples in wt. %

Mineral	SiO ₂	CaO	MgO	FeO	Fe ₂ O ₃	Al ₂ O ₃	MnO	Na ₂ O	K ₂ O	SO ₃	H ₂ O	CO ₂
Calcite	1.3- 2.4	47.6-50.1	0.8- 2.1	0.1 - 0.3	0.1 - 1.4	0.6- 1.1	0.1 -0.2	0.4 -0.1	0.02- 0.1	0.04- 0.2	0.2- 0.3	43.5-46.7
CaCO ₃												
Magnesite	1.4- 1.7	0.8- 1.4	41.0-45.1	0.05- 1.3	0.1 - 0.6	0.4- 1.1	-	0.1 -0.2	0.1 - 0.2	-	-	45.0-50.9
(crystalline)												
Magnesite	1.2- 2.4	0.9- 1.2	42.1-46.0	0.07- 0.3	0.08- 2.0	0.4- 0.7	-	0.1 -0.2	0.05- 0.1	0.03- 0.08	-	45.2-50.3
(amorphous)												
MgCO ₃												
Siderite	0.3- 1.4	0.6- 1.8	1.1-12.0	55.8 -59.9	0.1 - 2.7	0.2- 0.7	0.5 -1.0	0 - 0.1	0.1 - 0.2	-	-	30.3-35.8
FeCO ₃												
Dolomite	1.2- 1.6	30.1-32.7	20.4-21.8	0.05- 0.1	0.5 - 1.1	0.1- 1.7	0.02-0.5	0.05-0.1	0.1 - 0.2	0.02- 0.8	-	40.8-46.9
CaMg(CO ₃) ₂												
Kaolinite	44.9-45.3	0.2- 2.6	0.3- 0.4	0.07- 0.3	0.05- 2.3	37.0-38.1	-	0 - 0.1	0 - 0.1	0 - 0.1	13.1-14.3	-
Al ₂ O ₃ · 2SiO ₂ · 2H ₂ O												
Limonite	4.9- 5.3	0.1- 0.2	0.2- 0.4	-	80.8 -81.6	-	0.7 -0.8	0.1 -0.2	0.1 - 0.2	0 - 0.1	10.9-12.2	-
Fe ₂ O ₃ · 2H ₂ O												
Muscovite	44.1-46.0	0.4- 1.6	0.5- 2.1	0.2 - 0.9	1.7 - 2.1	36.1-37.3	0 - 0.1	0.1 -0.8	7.4 -11.3	0 - 0.1	4.1- 4.9	-
K ₂ O · 3Al ₂ O ₃ · 6SiO ₂ · 2H ₂ O												
Pyrite	0.1- 0.6	0.1- 1.3	0.2- 0.9	0 - 0.3	57.4 -59.5	0.5- 0.8	0 - 0.1	0 - 0.2	0.1 - 0.2	45.2 -47.1	-	-
FeS ₂												
Gypsum	0.1- 0.3	30.4-32.5	0.1- 0.6	0.1 - 0.6	0.4 - 0.6	-	0 - 0.1	0 - 0.2	0.1 - 0.2	44.8 -46.2	20.7-21.3	-
CaSO ₄ · 2H ₂ O												

Note: The TiO₂ and P₂O₅ contents were less than 0.1 wt. % for all minerals except muscovite, in which the TiO₂ was 0.2-0.5 wt. % and gypsum, in which the P₂O₅ was 0.2-0.4 wt. %.

The main purpose of the experimental technique used is the elimination of all possible diffusional complications. The experiments were carried out using a Derivatograph instrument (Hungarian Optical Works, Budapest). A dynamic inert atmosphere of purified N_2 with a flow rate of $5 \times 10^{-3} \text{ m}^3 \text{ s}^{-1}$ was used. The samples were arranged in a monolayer on the platinum multi-plate sample holder so that each sample particle was in contact with the holder. The sample mass M on one plate satisfied the condition $M \leq \rho Sd$ where S is the plate surface [4]. The sample mass was limited to 50 mg and the heating rate varied from 10 to 20 K min^{-1} .

Using these small samples and arranging them in a monolayer made it possible to eliminate the possible influence of evolved gas diffusion through the layer of the sample. Using a dynamic inert atmosphere made it possible to eliminate the outer diffusional complications, the "gas jacket" effect, around the decomposing single particle. It has been shown that heat transfer processes are not limited under similar conditions by [5]. Thus, the internal diffusion of evolved gas through a layer of solid reaction product on a single particle, is the only cause of possible diffusional complications, which may occur because of an increase in the layer thickness.

It was assumed that, for the smallest particles, the reaction proceeds in the kinetic region. The experiments were carried out under identical conditions; the diameter of the sample particles was successively increased. With respect to the increasing particle diameter, only the internal diffusion of evolved gas toward the surface of the single particles can influence the kinetics of the process under examination. A shift of the reaction into the transition region and its subsequent "dipping" into the diffusion region was estimated by the shift of the kinetic curves $\alpha = \alpha(T)$ towards the high temperature zone. This effect is caused by pore diffusion resistance and, therefore, by the decreasing reaction rate. Consequently, the time taken for the total process to proceed increases, and the final temperature of the reaction also increases, because of the linear heating rate.

Because the influence of other slowing factors has been eliminated, such a shift of the $\alpha = \alpha(T)$ curves can only be caused by the evolved gas diffusing through the porous layer of reaction product. This shift was recorded by the points of the reaction rate maximum and the final temperature. Hereafter, we will consider these temperatures as the characteristic temperatures of the reaction. With identical experimental conditions, the initial temperature of the reaction is approximately constant, because it is determined by the kinetics of the reaction which formed the cores of the particles, and by the change and growth which have taken place on the particle surface, which process is almost independent of particle size. For these reasons, we will not be concerned with the initial temperature of the reaction.

The diameter of the particles at which the increase in the final temperature or the increase in the temperature of the reaction rate maximum first becomes noticeable, was designated the critical diameter d_{cr} , from which the

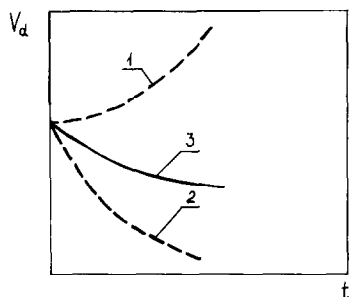


Fig. 1. Dependence of diffusion rate on time, in the case of diffusion in wide pores: 1, the diffusion rate is determined only by the increase in temperature; 2, the increase in thickness of the reaction product layer exerts an overwhelming effect on the diffusion rate; 3, the diffusion rate is determined by the increase in temperature and the thickness of the reaction product layer.

diffusional complications emerge, i.e. d_{cr} was designated as a boundary of the kinetic region.

Two opposing factors have an effect on the diffusion rate of evolved gas after the onset of the reaction; diffusion accelerates with temperature increase, but slows down when layers of reaction product grow on the particle surface. The diffusion rate behaviour depends on the temperature or time (it is not affected by the linear heating rate) and can be characterized by the plots on Fig. 1. In a general case, the influence of the growth of a reaction product layer is stronger than the effect of temperature increase and, therefore, V_d behaviour can be described by the total curve 3. The trend of curves 1 and 2 and, consequently, curve 3 depends on the temperature range of the reaction, the properties of the solid product layer, the dimensions of the crystals and of the pores formed, the properties of the evolved gases, etc. The region in which the thermal decomposition process proceeds is determined by the relationship between the chemical reaction rate V_r and the diffusion rate V_d (Fig. 2). If the diameter of the particles d is less than d_{cr} , then the reaction rate is always less than the diffusion rate and the total process proceeds in the kinetic region. When d is greater than d_{cr} (curve d_3), in the range $t_2 < t < t_3$, the diffusion rate is less than the reaction rate and the process proceeds in the diffusion region. At $t > t_3$, the process passes again into the kinetic region i.e. the decrease in the reaction rate becomes the dominant effect, not the decrease in the diffusion rate which is due to growth of the product layer. From $d > d_4$, there will be no reverse transition from the diffusion region to the kinetic region. It should be noted that the reaction rate maximum, or the region near it, is the most probable point of contact of the chemical reaction rate and diffusion rate curves.

Therefore, in contradistinction to a plane problem, in which the transition from the kinetic region to the diffusion region is determined only by the thickness of the product layer, in this problem everything is determined by a

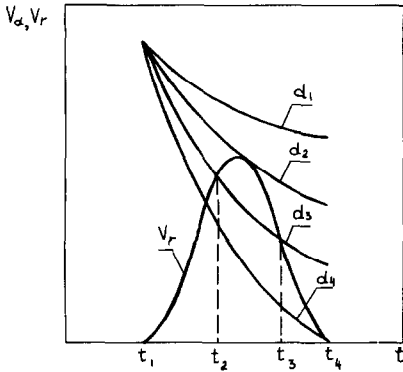


Fig. 2. Diffusion rate versus reaction rate relation, depending on the sample particle size: $d_1 < d_2 < d_3 < d_4$.

combination of the change in thickness of the product layer and the reaction rate. The most probable point of transition into the diffusion region is in the region of the reaction rate maximum. The critical diameter of the particles, above which diffusion complications begin to emerge, not the thickness of the product layer, is the main parameter, which it is necessary to determine.

It should be noted, that when the process proceeds in Knudsen's diffusion range, the diffusion rate $V_d \sim T^{1/2}$ and the deflection of the curve describing the diffusion (see Figs. 1 and 2) will change in the opposite manner. This produces some minor differences which do not, however, change the main conclusions.

RESULTS AND DISCUSSION

The critical particle dimensions for all the minerals studied are presented in Table 2. It is impossible to discuss all the results obtained in one paper. Carbonate minerals are of great importance in applied investigations; therefore only the results obtained for these minerals will be discussed here.

When studying the thermal decomposition processes of magnesite, usually only crystalline magnesite is studied, not the amorphous form. However, these two substances differ from each other, not only in terms of their crystallographic and physical properties, but also in their thermal behaviour.

The reaction interval we obtained for the thermal decomposition of crystalline magnesite is in good agreement with the works of other authors (see, e.g. [6]). It should be noted that cracking and sometimes self-crushing of the particles take place at the beginning of a reaction. In this case, coarse fragments are formed although their sizes are not changed during the reaction. It is easy to test this phenomenon by interrupting the experiment at the beginning of the reaction (at $T \approx 750$ K) and then bringing it to a conclusion. The size of the fragments is unchanged in both cases. The effect

TABLE 2

Critical particle dimensions and reaction interval ΔT for the minerals

Mineral	d_{cr} (μm)	d_{pr} (μm)	q (K min^{-1})	ΔT (K)
Calcite	200	400	20	255
Magnesite (crystalline)	400	600	10	173
Magnesite (amorphous)	600	1000	10	200
Siderite	1200	1500	10	140
Dolomite	200	1000	20	205
Limonite	720	1000	20	125
Kaolinite	1180	1200	20	270
Muscovite	100	100	20	227
Pyrite	250	300	20	254
Gypsum (dehydration)	200	400	20	50
Gypsum (dissociation)	250	300	15	285

of magnesite self-crushing was noted earlier [7]. The dependence of the characteristic temperatures of the reaction on particle sizes is presented in Fig. 3a. The thermal decomposition reaction of natural magnesite proceeds rather rapidly and its reaction interval is ~ 1.5 times smaller than the reaction interval for calcite. It would seem, therefore, that d_{cr} for magnesite would be smaller than for calcite. But the self-crushing phenomenon (which causes deep cracks to be formed in the particles, which greatly improves the diffusion conditions) leads to the fact that the d_{cr} for magnesite is twice that for calcite. With increasing particle size, the effect of diffusion on the thermal decomposition of magnesite is less than on the thermal decomposition of calcite. So for particles with an initial size of $d = 1500 \mu\text{m}$, the shift of the T_{max} curve is $\sim 27\text{--}28 \text{ K}$ (for calcite $\sim 37 \text{ K}$) and the shift of the T_f curve is $\sim 33 \text{ K}$ (for calcite $\sim 65 \text{ K}$). Although $d_{cr} = 400 \mu\text{m}$, even a 1.5 times size increase causes only a slight shift in the kinetic curves; this means that the kinetic constants for this reaction can be applied to considerably larger particles, as large as $d_{pr} = 600 \mu\text{m}$.

The thermal decomposition reaction of amorphous magnesite begins at $T \approx 683 \text{ K}$ which is about 70 K lower than for crystalline magnesite. The reaction temperature range (reaction interval) is wider for amorphous magnesite, than for the crystalline form and hence the chemical reaction rate for amorphous magnesite is less than for the crystalline one. This leads to a broadening of the kinetic region, which was corroborated by the experiments (Table 2). The kinetic region for amorphous magnesite is limited by $d_{cr} = 600 \mu\text{m}$, which is 1.5 times larger than d_{cr} for the crystalline form. It is interesting that the kinetic region expands, despite the fact that the self-crushing phenomenon was not observed and that CO_2 diffuses through the porous structure of MgO . This effect is possibly explained by the fact that the density of amorphous magnesite ($\rho = 2.9 \cdot 10^3 \text{ kg m}^{-3}$) is a little less than for the crystalline form ($\rho = 3.3 \cdot 10^3 \text{ kg m}^{-3}$) and, consequently, the porosity

of the product layer is higher in the case of the amorphous substance, thus improving diffusion conditions and, possibly, compensating for the absence of cracks. Moreover, the reaction rate is appreciably less, as was noted above.

The curves of reaction rate maximum temperature and final temperature (Fig. 3b) rise very slightly with increasing particle size. The shift in the curves is ~ 5 K for $d = 1000 \mu\text{m}$ and $\sim 7-8$ K for $d = 1200 \mu\text{m}$. It becomes greater at $d = 2000-2500 \mu\text{m}$, when the shift of the T_{max} curve towards the high temperature range is ~ 27 K and of the T_f curve is ~ 38 K at $d = 2500 \mu\text{m}$. The weak dependence of these curves on the particle sizes is caused, apparently, by the sloping trend of the diffusion rate curve (determined by the properties of the product layer), which slowly increases the diffusion region (Fig. 2) and, thus, leads to the sloping trend of the $T_{\text{max}} = T_{\text{max}}(d)$ and

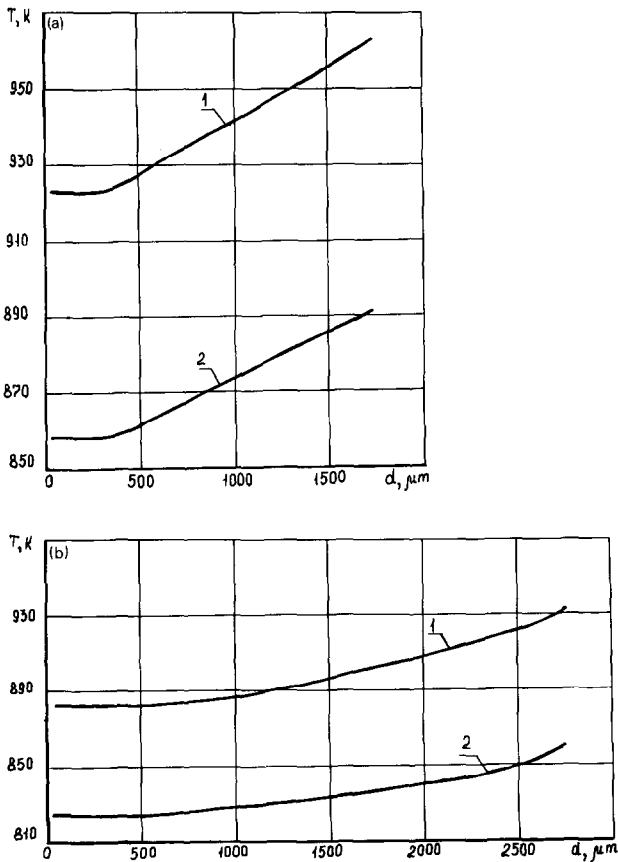


Fig. 3. Dependence of characteristic reaction temperatures on particle size for the thermal decomposition of a, crystalline magnesite; b, amorphous magnesite; c, dolomite; d, calcite. 1, T_f and 2, 3, T_{max} .

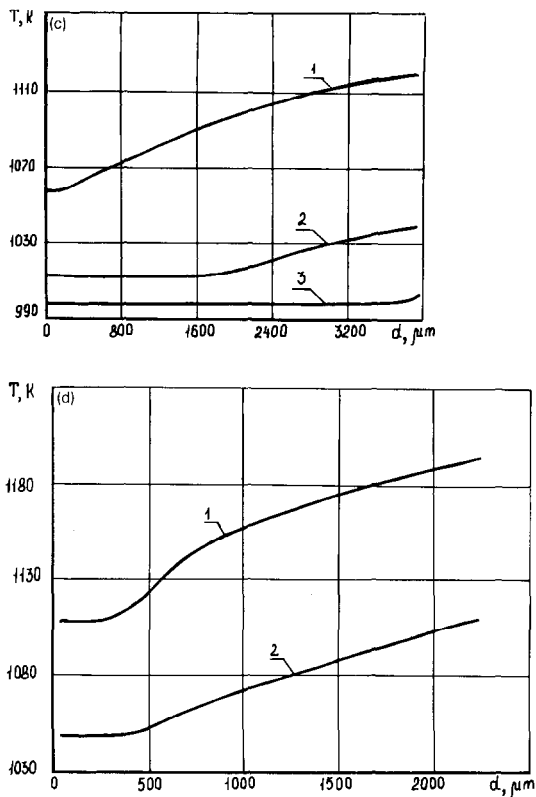


Fig. 3 (continued).

$T_f = T_f(d)$ curves. Thus, for practical calculations, it is possible to use the kinetic constants not only up to $d_{cr} = 600 \mu\text{m}$, but beyond to $d_{pr} = 600 \mu\text{m}$.

The thermal decomposition reaction of dolomite is characterized by three temperatures (apart from the initial temperature): the reaction rate maximum of magnesite dissociation, the reaction rate maximum of calcite dissociation and the final temperature. The temperature of the reaction rate maximum for magnesite as expected, is independent of particle size. This is connected with the fact that the dissociation pressure of magnesite at this temperature is about ~ 75 atm. The small temperature rise (Fig. 3c, curve 3) at $d = 4000 \mu\text{m}$ is apparently caused by experimental error, because the final fraction had the greatest spread of particle sizes. One can see in Fig. 3c that at first the diffusion complications have an effect on the final temperature of the reaction, i.e. the diffusion rate curves (Fig. 2) are very steep and intersect with the curve of the chemical reaction rate beyond the point of the rate maximum. We believe that this is connected with the screening of decomposed calcite crystals by the magnesium oxide crystals [1] and the superimposing actions of layers of magnesium and calcium oxides, which strongly inhibit the diffusion processes and determine the steepness of the diffusion

rate curve. Transition into Knudsen's diffusion region is also possible, and this reverses the deflection of the diffusion curve. If the boundary of the kinetic region is determined by the T_f curve, then $d_{cr} = 200 \mu\text{m}$. It should be noted, however, that practically the whole reaction proceeds in the kinetic region for the particles of considerably greater sizes. Thus, when $d = 1800 \mu\text{m}$, diffusion resistance begins to appear, affecting the $T_{\max}(d)$ curve behaviour at $\alpha_{\max} \approx 0.75$, i.e. 75% of the substance reacts in the kinetic region. Consequently the kinetic equations can be used for particle sizes considerably greater than $d_{cr} = 200 \mu\text{m}$. We believe that the kinetic constants can be used up to $d_{cr} \approx 1000 \mu\text{m}$, for practical engineering calculations.

Calcite has been extensively studied in many original works; therefore, we will only briefly discuss its dependence of reaction characteristic temperatures on particle size, see Fig. 3d. The final temperature is approximately constant up to $d \approx 200 \mu\text{m}$ and then increases with increasing d . The temperature of the reaction rate maximum is constant up to $d \approx 390 \mu\text{m}$. The diffusion rate curve is very steep and its intersection with the curve of the chemical reaction rate takes place either in the rate maximum region or after it. Therefore, the duration of the diffusion region, up to the rate maximum, tends to zero and the diffusion complications have an effect only on the $T_f(d)$ curve and subsequently, when the diffusion range increases, the $T_{\max}(d)$ curve also shifts. With increasing particle size, the $T = T(d)$ curves become more sloping. From our point of view, this can be explained by the fact that the number of cracks in the product layer, covering the reacting particle, increases with particle size increase. This phenomenon can be confirmed by examining the particles after the experiments. These cracks simplify the diffusion process and partly compensate for the growth of the reaction product layer.

Apparently, $d_{cr} \approx 200 \mu\text{m}$ may be considered to be the boundary of the kinetic region, but taking into account the fact that the diffusion complications have an effect on the T_{\max} curve from $d \approx 400 \mu\text{m}$ only, and $\alpha_{\max} \approx 0.76$, i.e. much of the substance reacts in the kinetic region in this case too, in all probability, it is possible to assume that $d_{pr} \approx 400 \mu\text{m}$ is the boundary of the kinetic region for practical engineering calculations.

The characteristic temperatures and the kinetic region of the thermal decomposition of siderite, as a function of the single particle size, have been described by us in ref. 4.

We have conducted similar investigations for all the other minerals present in the mineral matter of solid fuels. The results are presented in Table 2. Unfortunately, it is impossible to analyse all this data in one paper and therefore we have limited our discussion of the results to those which are most interesting from our point of view.

ACKNOWLEDGEMENT

The author wishes to thank Professor Yu.A. Rundygin for valuable discussions and his great attention to this work.

REFERENCES

- 1 D. Young, *Decomposition of Solids*, Pergamon Press, Oxford, 1966.
- 2 W.W. Wendlandt, *Termicheskie Metody Analiza*, Moscow, Mir, 1978 (in Russian).
- 3 M.E. Brown, D. Dollimore and A.K. Galwey, in C.H. Bamford and C.F.H. Tipper (Eds.), *Comprehensive Chemical Kinetics*, Vol. 22, *Reactions in Solid State*, Elsevier, Amsterdam, 1980.
- 4 V.Yu. Zakharov and Z. Adonyi, *Thermochim. Acta*, 102 (1986) 101.
- 5 V.V. Aleksandrov and V.V. Boldyrev, *Izv. Sib. Otd. Akad. Nauk SSSR, Ser. Khim. Nauk.*, 4(9) (1974) 59 (in Russian).
- 6 N.D. Topor, *Differentsialno-Termicheskii i Termovesovoi Analiz Mineralov*, Nedra, Moscow, 1964 (in Russian).
- 7 E.A. Prodan, M.M. Pavlyuchenko and S.A. Prodan, *Zakonomernosti Topokhimicheskikh Reaktsii*, Nauka i Tekhnika, Minsk, 1976 (in Russian).